

Article

Research on the Tribological Behavior of Textured Cylindrical Roller Thrust Bearings with Different Distributions of Pits and Nylon Cages under Dry Condition

Yazhe Chen ¹, Risheng Long ^{2,*} , Zhihao Jin ², Chen Zhao ² and Ming Wang ³¹ School of Mechanical Engineering and Automation, Northeastern University, Shenyang 110819, China² Equipment Reliability Institute, Shenyang University of Chemical Technology, Shenyang 110142, China³ China Construction Industrial & Engineering Group Co., Ltd., Nanjing 210023, China

* Correspondence: etomi@163.com

Abstract: Differing from the published documents on the effect of texture distributions of sliding tribo-pairs on their friction and wear properties, this study introduced eight patterns to reveal the influence of different distributions of pits on the tribological behavior of textured rolling element bearings with nylon cages under dry condition, namely: Outside-1/4 (OS1/4), Outside-1/2 (OS1/2), Outside-3/4 (OS3/4), Inside-1/4 (IS1/4), Inside-1/2 (IS1/2), Inside-3/4 (IS3/4), Bothside-1/3 (BS) and full (FP). A fiber laser marking system was used to prepare them on the raceways of the shaft washers of cylindrical roller thrust bearings (81107TN). A vertical universal wear test rig was used to obtain their coefficients of friction under an axial load of 2600 N and a rotating speed of 250 RPM, without any lubricant provided. Their wear losses and worn surfaces were characterized. The influence mechanism of different distributions on the tribological properties was also discussed. The results show that the self-lubricating performance of nylon cages can ensure the continuous operation (≥ 5 h) of cylindrical roller thrust bearings under dry condition. The influence of outside-distributed patterns on the friction and wear properties of bearings is significant. The friction-reducing effect and wear resistance of full textured group is improved but not the best. The friction-reducing and anti-wear behavior of OS1/2 is similar to that of FP. In this work, OS3/4 can provide the best tribological performance under self-lubricating conditions. Compared with the data of smooth bearings, its average coefficient of friction and wear loss can be reduced by 37.68% and 38.85%, respectively. This work would provide a valuable reference for the raceway design and reliability optimization of rolling element bearings.

Keywords: rolling element bearing; tribological behavior; surface texture; distribution of pits; self-lubricating nylon cage



Citation: Chen, Y.; Long, R.; Jin, Z.; Zhao, C.; Wang, M. Research on the Tribological Behavior of Textured Cylindrical Roller Thrust Bearings with Different Distributions of Pits and Nylon Cages under Dry Condition. *Lubricants* **2023**, *11*, 154. <https://doi.org/10.3390/lubricants11040154>

Received: 9 February 2023

Revised: 20 March 2023

Accepted: 21 March 2023

Published: 23 March 2023



Copyright: © 2023 by the authors. Licensee MDPI, Basel, Switzerland. This article is an open access article distributed under the terms and conditions of the Creative Commons Attribution (CC BY) license (<https://creativecommons.org/licenses/by/4.0/>).

1. Introduction

In a highly developed modern society, the generation, manufacturing and transportation of power are central industrial activities, which all rely on the involvement of moving parts and interacting surfaces [1]. In order to realize the reliable and long-term employment of such machines, the friction and wear on interacting surfaces should be enhanced. In fact, the tribological behavior of those surfaces is mainly influenced by surface characteristics (e.g., roughness, hardness and topography), contact type, lubrication regime, loads, lubricant, as well as materials [2–4].

Surface characteristics and materials are the only two factors that can be customized according to individual requirements or specific conditions among all of the above-mentioned, partially or entirely. Surface texture (ST) can create periodically distributed macro-/micro-units (e.g., pillar, pit, groove and grid) on the target surfaces in a geometry or pattern to tune their tribological properties. During surface texturing processing, there is no external element added [5–15]. The published works on the different distributions of textured units

or local-distributed texture patterns are all focused on the journal bearings by now [16–20]. Morris et al. studied the micro-hydrodynamic and friction behavior of chevron-based textured patterns under low loads (12.4 N) and reciprocating sliding conditions. They also proposed a method that combined numerical and experimental research to determine the beneficial effect of pressure disturbance caused by micro-hydrodynamics on the lubricant reservoir trapped in the textured cavity and the improved micro-wedge flow. Their results show that low sliding motion textured surfaces of suitable geometry, pattern and distribution can induce micro-hydrodynamic pressure perturbations, thus enhancing lubricant film thickness. Lubricant retention in the created micro-reservoirs, as well as pressure perturbations at the inlet conjunction, can result in differing extents of effective micro-wedge effect. The texture pattern and distribution can be optimized for given conditions, dependent on the intended application under laboratory conditions, and near optimal conditions may suffice for most application areas [21]. Rahmani R. et al. examined the performance of partially textured sliding surfaces with rectangular and triangular features. To obtain optimum texture characteristics for maximum load carrying capacity, they outlined an approach to obtain a set of global optimum design parameters for partially textured surfaces. Their analysis shows that the performance of a textured surface deteriorates as the number of features increases. The optimum performance can be achieved when approximately between two-thirds and three-quarters (depending on the feature shape) of the overall contact domain is textured [22]. Vlădescu S. C. et al. fabricated three texture configurations on the surface of shell components to research the impact of surface texturing on the friction of crankshaft bearings and found that the full textured shells showed a substantial reduction of friction (approximately 18%) compared with the non-textured reference. Friction reductions of up to 13% were observed using shells that were only textured outside the loaded region [23].

The related research on rolling element bearings (REBs) has not been reported yet. Cylindrical roller thrust bearings (CRTBs) are commonly used to bear huge axial force and limit the axial displacement of shafts in rotating tools or devices, such as impact hammers, electric screwdrivers, universal wheels, machine tools, etc. Due to their unique separability, CRTBs are also used to research the influence of surface texturing on the tribological performance of rolling element bearings. The bearings may be cheap, but their failures, caused by contamination, poor lubrication, wrong fits, misalignments, etc., are costly. Rosenkranz A. et al. fabricated dots on the raceways of washers of 81212 bearings (SAE 52100) with a periodicity of 6.5 μm and a depth of 1 μm , and finally obtained an 83% reduction of the wear loss of the textured bearing compared with that of a smooth reference [24]. Long R.S. et al. also researched the influence of different texture units (pits, grooves and leaf-veins) on the tribological behavior of 81107TN bearings [2,25–29]. However, the effect of the distribution of units on the friction and wear performance of rolling element bearings is still unclear, especially under dry condition [30].

Obviously, roller element bearings operating without any lubricant (either oil or grease) is very uncommon and can only be the case for extreme operating conditions (temperature and vacuum) or cleanliness requirements. Even in these cases, usually a solid lubricant, such as graphite, DLC or 2D material coatings (e.g., MoS_2 , graphene, MXenes, etc.) is employed [31,32]. In our previous trials, an 81107 bearing with a copper cage was tested to reveal its tribological behavior under a vertical load of 2600 ± 100 N and a rotating speed of 250 RPM, without any lubricant. When the test started, the temperature of the bearing rose very fast and it was quickly blocked, leaving a lot of copper powder in the cavity of the tribo-pair. However, the result was different in the case of nylon cages [33]. Due to the good self-lubricating performance of nylon, the 81107TN (YFB, Changzhou, China) bearings with nylon cages kept running for more than 5 h under the same conditions, without cage fracture or roller blocking phenomena. Therefore, based on previous works [2,25–29], and differing from the textured sliding tribo-pairs in Refs. [21,22] and coatings used in Refs. [31,32], eight distributions of pits were manufactured on the shaft washers of 81107TN bearings with self-lubricating nylon cages and tested to obtain their

coefficients of friction (COFs) using a vertical universal tribo-tester under dry condition, i.e., without any lubricant provided. The mass losses and worn surfaces of shaft washers (both textured and smooth) were measured and characterized. The influence mechanism of the distributions of pits on the friction and wear properties of cylindrical roller thrust bearings was also discussed. This work would provide a valuable reference for the raceway design and reliability optimization of rolling element bearings.

2. Materials and Modeling

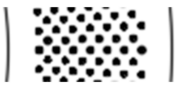
The sketch of the 81107TN bearing can be found in Ref. [25]. The diameter of the inner hole of shaft washer is 35 mm. The diameter of the inner hole of housing washer is 37 mm. The outer diameters of the shaft washer and housing washer are 52 mm, with the same thickness of 3.5 mm. The diameter and height of rollers are 5 mm. Among all parts, the shaft washer, housing washer and rollers are fabricated by GCr15 (SAE 52100). Their hardnesses are about HRC 60 ± 1 and their surface roughness is about $0.8 \mu\text{m}$. The cage is made of nylon (PA66, Black).

The pits are prepared on the raceways of shaft washers using a fiber laser marking system. The parameters of fiber laser marking system (PL100-30W, Sepbase, Shenyang, China) include: laser power, 30 W; scanning speed, 100 mm/s; and frequency, 72 kHz. The laser wavelength is $1064 \mu\text{m}$. The dimensions of the pits in this work are all the same: the diameter is $300 \mu\text{m}$ and the depth is $15 \mu\text{m}$. Through repeated trials, the circumferential interval angle is set to 1.5° and the distance between two adjacent pits is set to 0.89 mm (see Figure 1a). According to the distributions of pits, there are eight patterns introduced: Outside-1/4, Outside-1/2, Outside-3/4, Inside-1/4, Inside-1/2, Inside-3/4, Bothside-1/3 and full. They are coded as OS1/4, OS1/2, OS3/4, IS1/4, IS1/2, IS3/4, BS and FP, respectively (see Table 1). A group of smooth bearings are introduced as a reference and coded as SS. To eliminate the human and uncertain factors during wear tests, the wear tests of each pattern were repeated three times using three bearings. Thus, the total number of bearings consumed is 27.

Table 1. Groups of 81107 bearings with different distribution patterns.

Sample No.	Pattern	Area Density (%)
S1/4		2.19
OS1/2		4.38
OS3/4		6.57
IS1/4		2.19
IS1/2		4.38
IS3/4		6.57
BS		5.80

Table 1. Cont.

Sample No.	Pattern	Area Density (%)
FP		9.49
SS		—

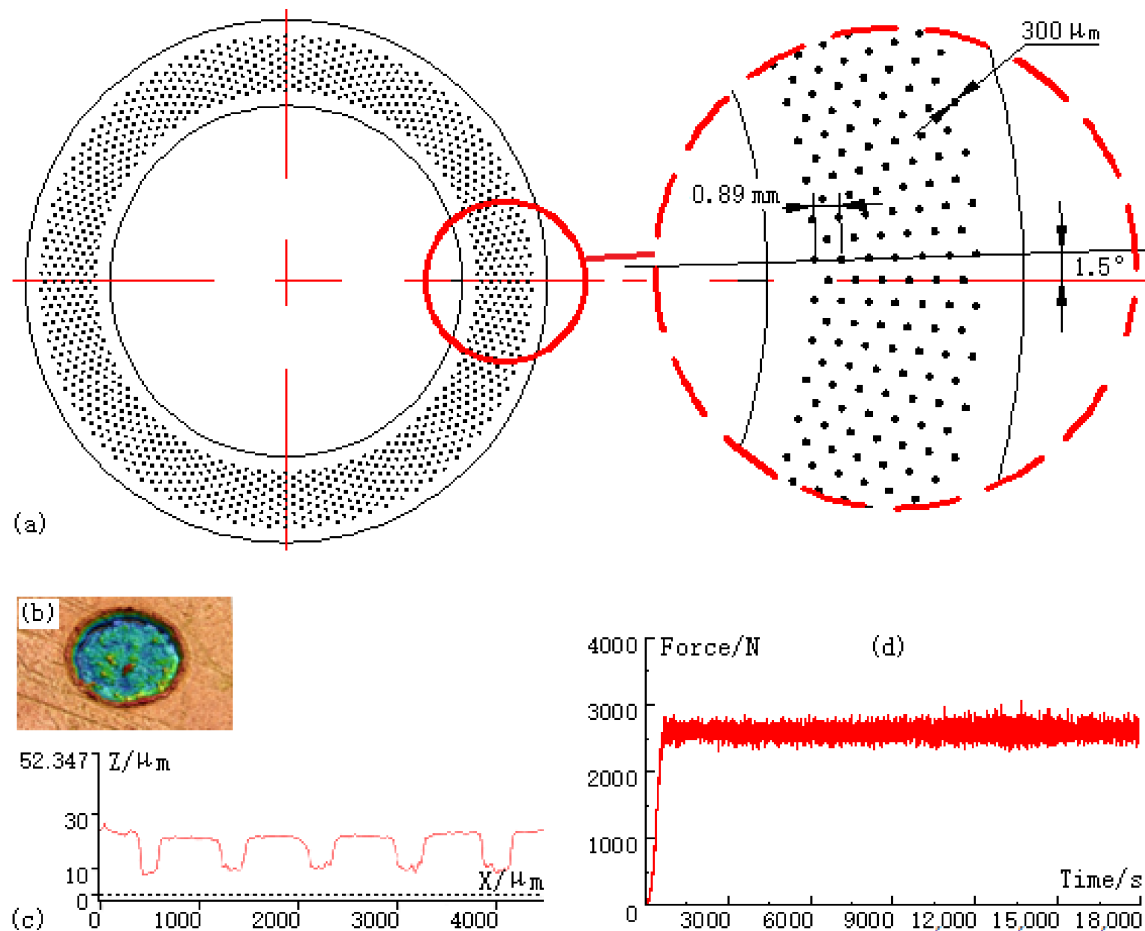


Figure 1. Sketch of pit parameters, characteristics of pits and the applied force-time curve. (a) Sketch of pit parameters; (b) 3D image of pit unit; (c) profile of pits; (d) force-time curve applied during wear test.

Note that the antirust oil on the shaft washer must be removed before marking. Prior to each wear test, the following pre-treated procedures should also be conducted: first, polish the textured shaft washers with sandpapers (from 800# to 2000# grades) to remove the micro-bulges along the edges of pits (see Figure 1b,c); second, clean the polished washers in an ultrasonic cleaner (VGT-1620QTD, China) for 15 min, and dry them using a hot-air blower. A vertical universal wear test rig (MMW-1A, Huaxing, Jinan, China) was used to research the tribological properties of bearings using a customized tribo-pair (see Figure 2) under a vertical load of 2600 ± 100 N and a rotating speed of 250 RPM, without any lubricant provided [21]. The room temperature is 22 ± 1 °C and the humidity is $35 \pm 5\%$. In this work, 2600 ± 100 N and 250 RPM are a combination determined by repeated trials and can ensure that all groups may complete their tests and have obvious

variations in their COF curves. The duration of each test is 18,000 s, which is dependent on the maximum sampling number of wear test rig.

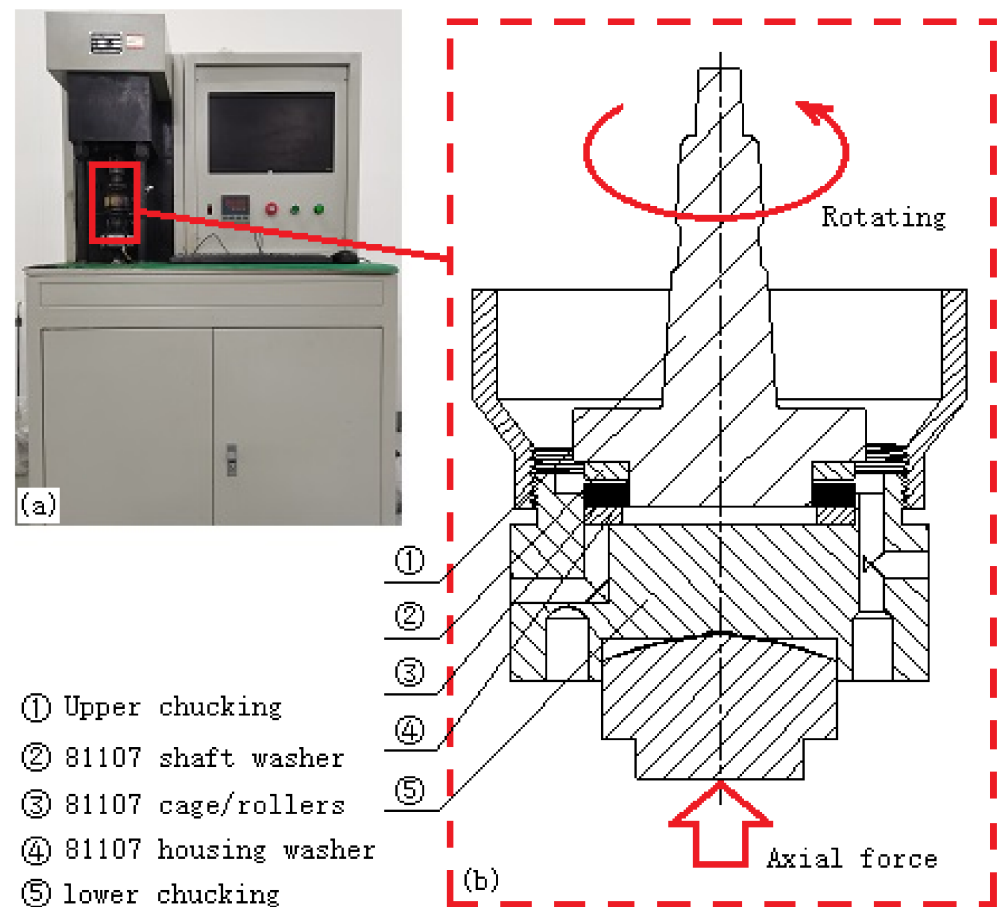


Figure 2. Photo of MMW-1A tribo-tester and sketch of the customized tribo-pair for 81107 bearings. (a) MMW-1A tribo-tester; (b) tribo-pair for 81107 bearings.

When one test was finished, prior to mass measurement, the shaft washer was cleaned in the ultrasonic cleaner for 15 min and then dried with hot air. An electronic analytical balance (EX225D, Ohaus, Parsippany, NJ, USA) with a precision of 0.1 mg (0.01 mg readability) was used to measure the mass of the shaft washer before and after testing. The difference between the measured weight before and after is the wear loss of the shaft washer.

3. Experimental Results

3.1. COFs and Wear Losses

The COF curves of cylindrical roller thrust bearings with self-lubricating nylon cages under dry condition are shown in Figure 3. To easily compare the differences among the groups, the curve of SS is also added as a reference. Note that each COF curve in the figure is the average curve of three tests of three bearings. Evidently, the curves in Figure 3 are quite different from those in Ref. [26], i.e., there is no stable-running period. When one test started, the curve quickly climbed and then entered a relatively stable stage, similar to the loading curve in Figure 1, whether or not it was textured or smooth. When comparing the curves in Figure 3a–f, it is easy to find that the COF curves of some textured groups (e.g., OS1/2, OS3/4, BS and FP) are evidently lower than that of the smooth reference.

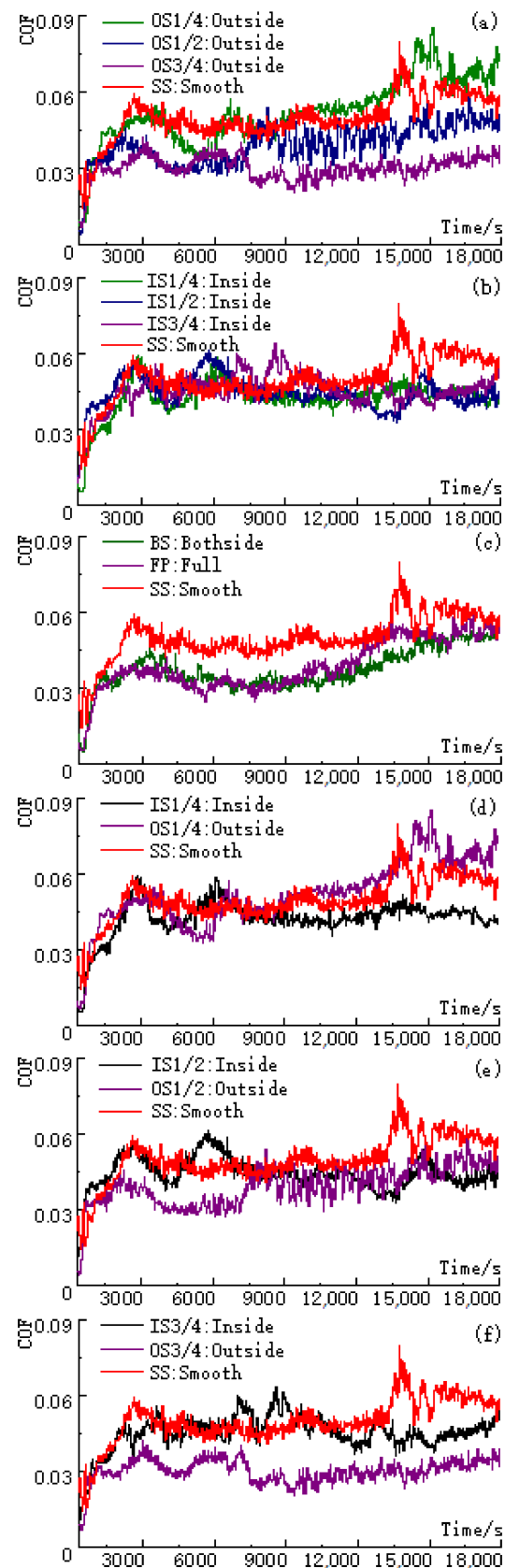


Figure 3. COF curves of cylindrical roller thrust bearings with self-lubricating nylon cages under dry condition. (a) Outside patterns (OS1/4, OS1/2 and OS3/4); (b) inside patterns (IS1/4, IS1/2 and IS3/4); (c) BS and FP; (d) OS1/4 and IS1/4; (e) OS1/2 and IS1/2; (f) OS3/4 and IS3/4.

The average COFs and wear losses of the nine patterns are shown in Figure 4. The error bars are a little large, which reflect the fluctuation of the effect of different distribution patterns on the wear resistance and friction-reduction performance of rolling element bearings under dry condition. Considering that the wear tests of each pattern were repeated three times with three bearings (curves with significant differences were removed and supplementary tests were conducted), the mean value in Figure 4 are statistically significant and comparative. Note that the average COF of each pattern is the sum of the values of each COF curve at each sampling point in Figure 3 divided by the total number of sampling points. As shown in the Figure 4a, the average COFs of pit textured groups are almost all lower than that of the smooth one, except for OS1/4, thus indicating the obvious friction-reducing effects of texture patterns. Specifically, the average COF of OS3/4 is the lowest. The average COFs of OS1/2, BS and FP are almost the same and significantly lower than that of the smooth group. The average COFs of inside groups (IS1/4, IS 1/2 and IS3/4) are close to each other and higher than those of OS1/2, BS and FP.

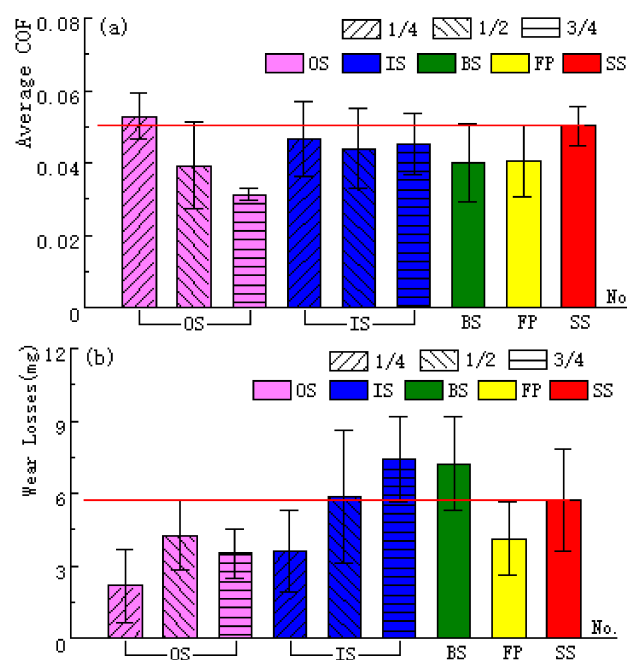


Figure 4. Average COFs and mass losses of cylindrical roller thrust bearings with self-lubricating nylon cages under dry condition. (a) Average COFs; (b) wear losses.

The mass losses of the shaft washers of the nine patterns are compared in Figure 4b. The loss of the smooth group is also added as a reference. Note that the mass loss of each group is the average of nine measurements of three tests of three bearings. Apparently, the wear losses of most pit textured groups are significantly lower than that of the smooth reference, except for IS1/2, IS3/4 and BS. Specifically, the mass loss of OS1/4, 2.17 mg, is the lowest among all of the patterns. Compared with the loss of SS (5.74 mg), its anti-wear performance improves by 62.20%. The wear losses of OS3/4 and IS1/4 are close and equal to 3.51 mg and 3.61 mg, respectively. The mass losses of OS1/2 and FP are also very close (4.26 mg and 4.13 mg), but higher than those of OS3/4 and IS1/4. The losses of BS and IS3/4 are 7.42 mg and 7.21 mg, which are quite higher than that of the smooth reference, respectively. By comprehensively comparing the COF curves, average COFs, and wear losses of all groups, OS3/4 can provide the best friction-reducing performance and wear resistance, which can be improved by 37.68% and 38.85%, respectively. In contrast, the friction-reducing and anti-wear properties of FP are only improved by 19.37% and 28.05%, compared with the data of the smooth group respectively. The friction-reducing and anti-wear behavior of OS1/2 is similar to that of FP and is better than that of SS by 21.72% and 25.78%.

3.2. Worn Surfaces

The unclean worn surfaces of the shaft washers of the nine groups are shown in Figure 5. Obviously, there is an apparent film left on the raceway in each group, especially in IS1/2, IS3/4, FP and SS. The material of the residual film has been checked and identified using the Fourier transform infrared spectroscopy (FTIR, IS10, Thermo Fisher Scientific, Waltham, MA, USA) in Ref. [26]. The obvious infrared characteristic spectrum of nylon was observed. Under the centrifugal force of the high-speed rotation of the shaft washer, there is almost no nylon powder left in the pits inside the raceway (see Figure 5g–h) [34]. The nylon film is mainly concentrated on the outside of raceway. There is also an apparent nylon powder stacked in the outside-distributed pits and some are even completely covered by nylon film or powder, especially in Figure 5b,c,g.

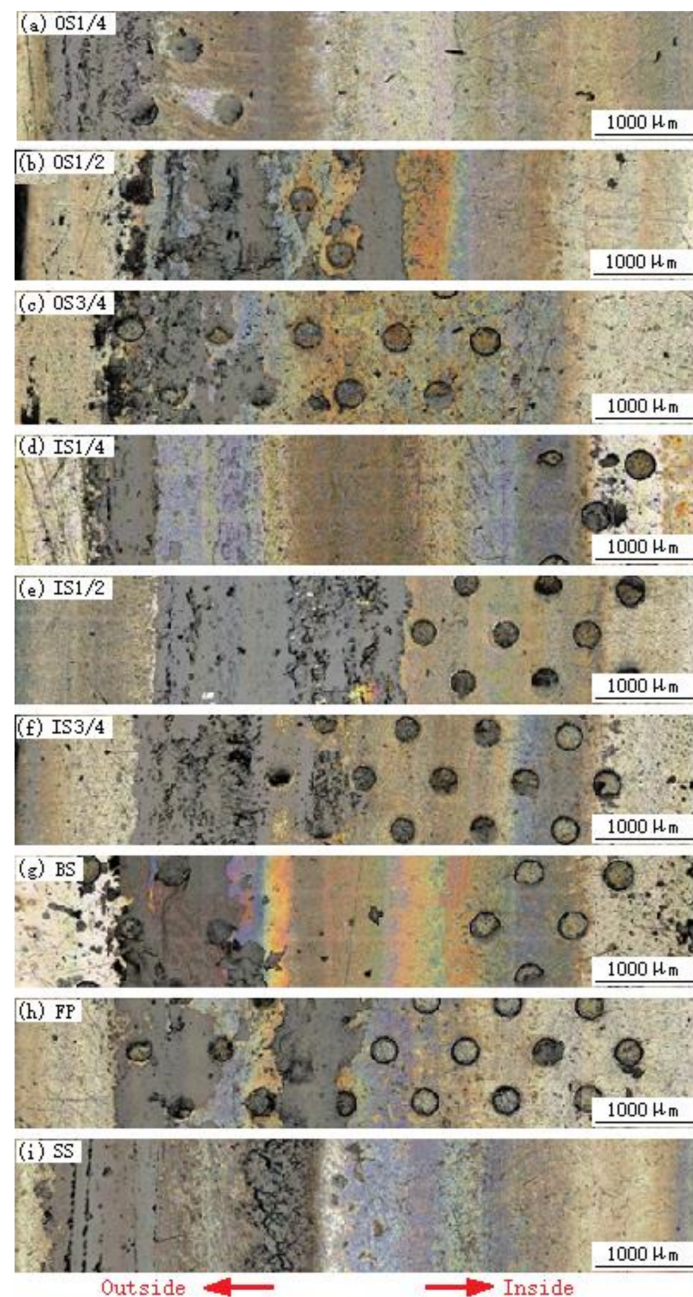


Figure 5. Unclean worn surfaces of the shaft washers of cylindrical roller thrust bearings with self-lubricating nylon cages under dry condition. (a) OS1/4; (b) OS1/2; (c) OS3/4; (d) IS1/4; (e) IS1/2; (f) IS3/4; (g) BS; (h) FP; (i) SS.

The clean worn surfaces of the shaft washers are shown in Figure 6. Apparently, there are high-temperature marks existing on their raceways, both textured and smooth. The ablation phenomena of IS1/4 and BS are particularly serious. Based on the worn surfaces, the wear pattern of cylindrical roller thrust bearings in this work is mainly abrasive wear combined with fatigue pitting.

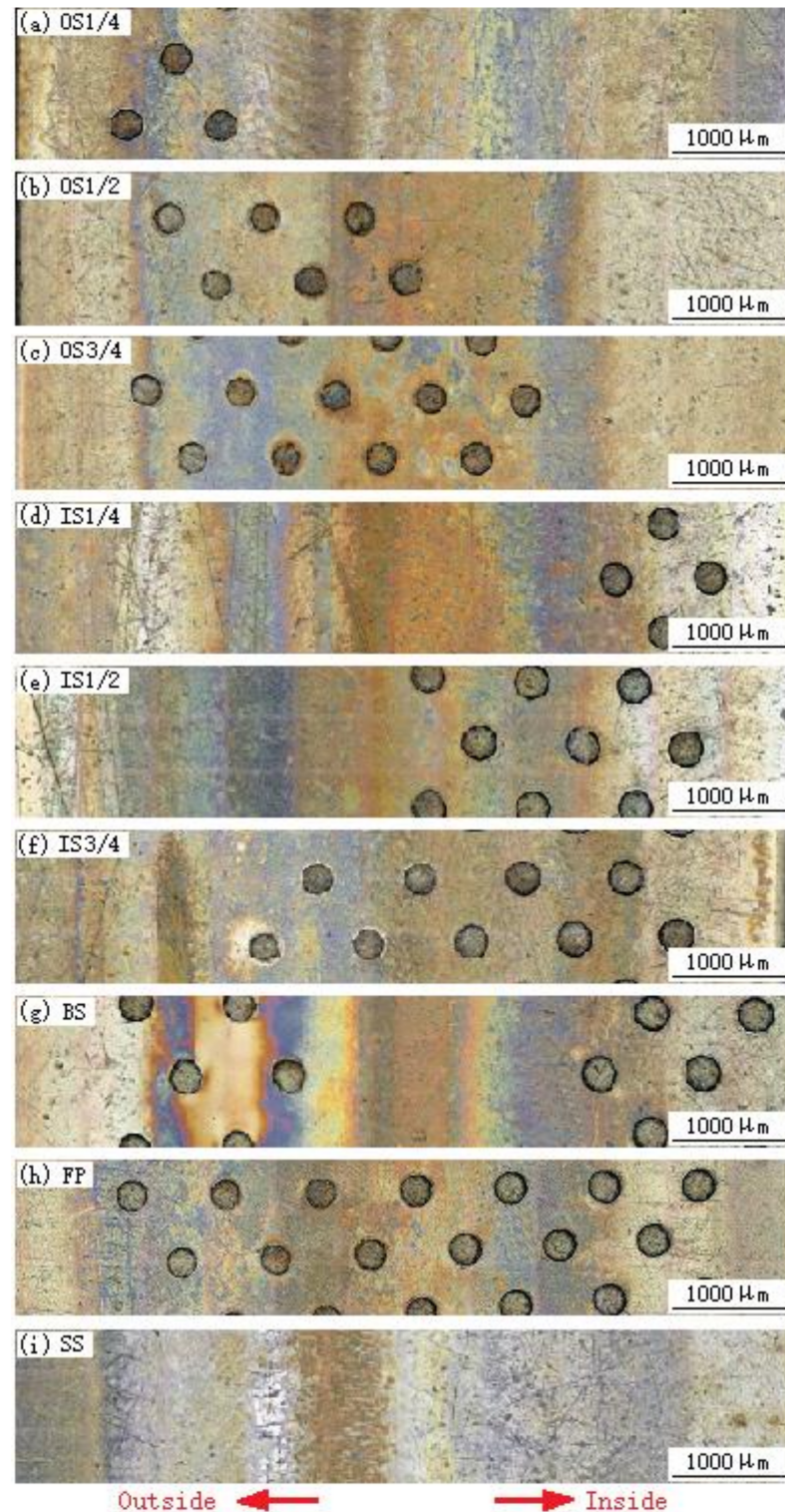


Figure 6. Clean worn surfaces of the shaft washers of nine groups. (a) OS1/4; (b) OS1/2; (c) OS3/4; (d) IS1/4; (e) IS1/2; (f) IS3/4; (g) BS; (h) FP; (i) SS.

4. Discussions

4.1. Effect of the Distributions of Pits on the Tribological Behavior of Rolling Element Bearings

When the pits are distributed on the outsides of raceways, as shown in Figure 3a, the COF curves of OS1/2 and OS3/4 are obviously lower than that of the smooth group. The curve of OS1/4 is mixed with that of SS and is hard to distinguish. When the pits are on the insides of the shaft washers (see Figure 3b), the three COF curves of IS1/4, IS1/2 and IS3/4 are mixed with that of the smooth reference, which is a little higher. It is difficult to distinguish the difference between them.

Similarly, as shown in Figure 3d, when the widths of the patterns are only 1/4 of the raceway, the curves of IS1/4 and OS1/4 are mixed at the beginning and gradually separate from the 9000th s. In the latter half of the wear tests, the curve of OS1/4 is the highest, and that of IS1/4 is the lowest. When the widths of the patterns are 1/2 of the raceway, the curves of OS1/2 and IS1/2 are easily distinguished at first but become mixed in the latter period (see Figure 3e). The curve of OS1/2 is completely below that of the smooth reference. When the widths of the patterns are 3/4 of the raceway, the curve of OS3/4 is significantly lower than that of the smooth group during the whole test (see Figure 3f). The curve of IS3/4 is mixed with that of SS but gradually lowers from the 12,000th s. The 3D worn surfaces (with 8000% enlargement in height direction) and section profiles of the shaft washers of BS, FP, OS1/2, OS3/4, IS1/4 and SS are shown in Figure 7. Obviously, the depth of the furrows of OS3/4 and IS1/4 are apparently shallower than those of the other groups.

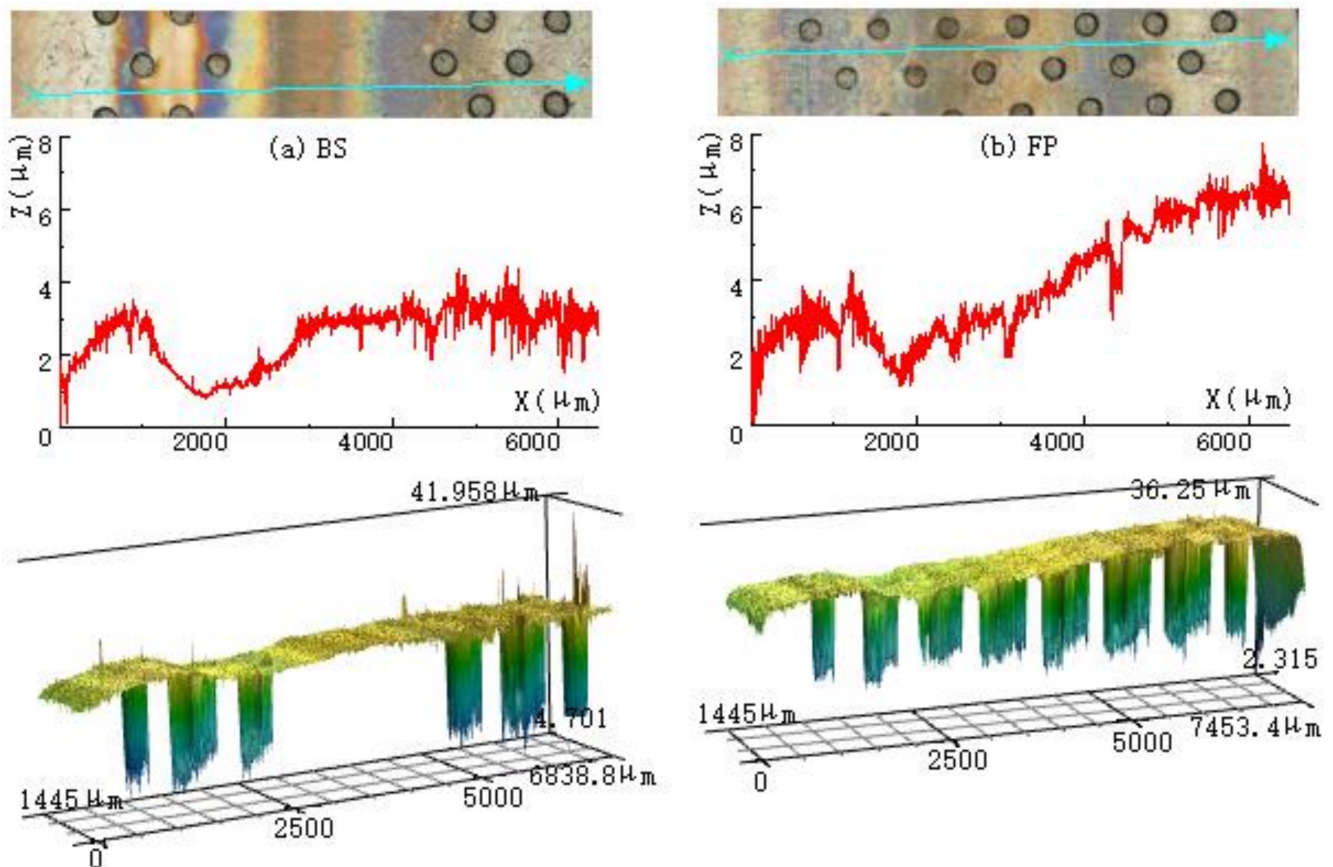


Figure 7. Cont.

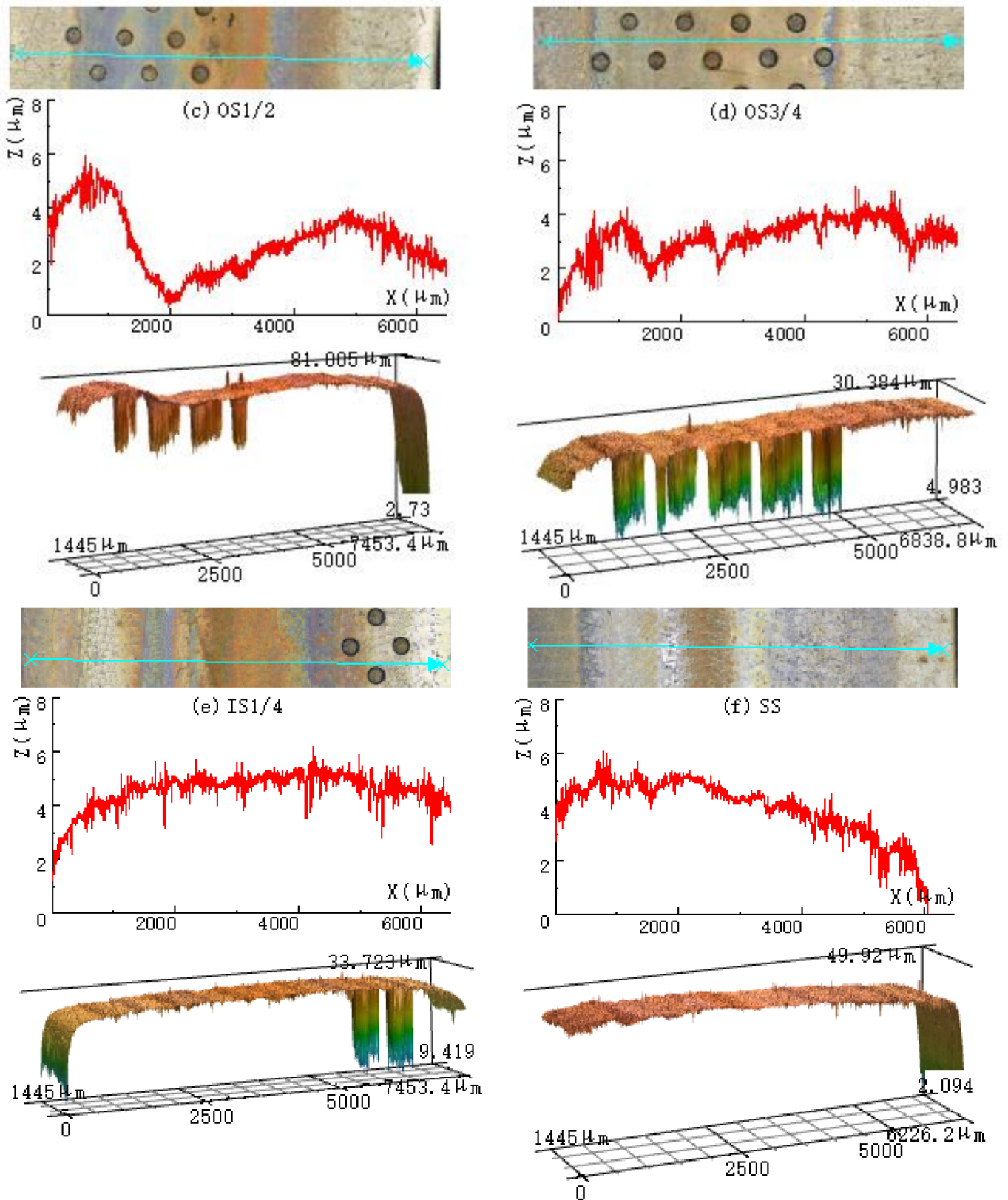


Figure 7. 3D worn surfaces (8000% enlargement in height direction) and section profiles of the shaft washers. (a) BS; (b) FP; (c) OS1/2; (d) OS3/4; (e) IS1/4; (f) SS.

In regard to the full textured pattern (FP) and BS, their COF curves mix together and are difficult to distinguish (see Figure 3c). Furthermore, as shown in the figure, their curves

are obviously lower than that of the smooth group. This is consistent with their average COFs in Figure 4a.

The mass loss of OS1/4 is the lowest among all of the groups. Compared with the data of the smooth reference, its anti-wear performance is improved by 62.20% (see Figure 4b). When the pits are distributed on the outsides of raceways, the anti-wear properties of three patterns (OS1/4, OS1/2 and OS3/4) are significantly improved. When the pits are on the insides of raceways, the mass loss of IS1/4 is apparently reduced. The wear behavior of IS1/2 is slightly worse than that of the smooth reference. The wear resistance of IS3/4 is the worst among all of the groups. The width of distribution has a great influence on the wear resistance of bearings. For the three outside-distributed groups, i.e., OS1/4, OS1/2 and OS3/4, their anti-wear properties deteriorate at first and then improve with the increase in width.

In this work, the friction-reducing effect and wear resistance of full textured pattern (FP) is not the best under a self-lubricating condition. Compared with the data of the smooth reference, the friction-reducing and anti-wear properties of FP are improved by 19.37% and 28.05%, respectively. OS3/4 can provide the best comprehensive friction-reducing and anti-wear properties, which can be enhanced by 37.68% and 38.85%, respectively.

4.2. Influence Mechanism of the Distributions of Pits on the Tribological Behavior of Rolling Element Bearings with Self-Lubricating Nylon Cages under Dry Condition

The influence of the distributions of the pits on the friction and wear properties of rolling element bearings with self-lubricating nylon cages under dry condition can be listed as follows: (1) when one rolling bearing is tested without any lubricant, for the direct contact between the rollers and the pockets of nylon cage, there is a large amount of nylon powder generated. Owing to the centrifugal force during the high-speed rotation of the shaft washer, the nylon powder will move along the radius direction, from the inside to the outside [34]. This will significantly increase the rolling resistance of the “washers-cage-rollers” system and cause the rapid rising of the temperature of the bearing [2,25–29]. Under the combined action of the fast-rising system temperature, local contact flash-temperature, and centrifugal force, a nylon film gradually forms near the outside of the raceway of the shaft washers (see Figure 5), both textured and smooth. This is the reason why the bearings with nylon cages can run for a long time without any lubricant, but those with copper cages cannot. Due to the relatively higher COF between a nylon–steel tribo-pair than that between a steel–steel pair, as well as the mechanical properties of nylon, the COF curve of bearing will increase quickly, but its wear loss may be reduced (see Figure 3). (2) Pits can effectively collect and hold debris, whether it is metal abrasive particles or nylon powder. Compared with the smooth bearings, the amount of debris left on the raceway can be significantly reduced, which is why the COF curves of most pit textured bearings are obviously lower than that of the smooth reference. In the meantime, pits can effectively reduce the contact stresses of the bearing, especially those points between the two ends of the rollers and raceway. This is another reason for the lower average COFs of most textured groups. Although the pits on the inner side can store nylon powder and metal debris, it is not conducive to their radial movement, especially for IS3/4, which is the reason for its higher mass loss compared to those of the other groups. This is also the reason for the excellent friction and wear properties of outside groups (OS1/4, OS1/2 and OS3/4). As shown in Figure 4, the tribological performance of full textured bearings can be considered as the synthesis and balance of the OS1/4 and IS3/4 groups. (3) In this work, when the dimensions of pits are fixed, the higher the area ratio is, the larger the effective volume is. As a result, the debris storage capacity will be significantly enhanced. Meanwhile, the larger area ratio also means a reduced effective contact area. The frictional resistance of the “washers-cage-rollers” system will increase and the stress concentration along the edges of pits will become serious. This will further cause the apparent peeling off of material and obvious “edge crushing” phenomena of pits. The metal debris generated may drop into the cavity of the tribo-pair or melt into the nylon film and remain in the “washers-cage-rollers”

system. What is left in the system will deteriorate the friction and wear performance of bearings, especially during its radial movement, and should be held responsible for the high wear losses of IS1/2, IS3/4 and BS [2,25]. (4) Compared with the partial textured groups, the full textured pattern has the largest capacity to collect and store debris, but it also seriously hinders the radial movement of wear debris, which is why the tribological behavior of OS1/4, OS1/2 and OS3/4 are superior to that of FP. The local un-textured region can change the radial moving mode of the debris, whether from the textured region to the smooth one or from the smooth area to the textured area, thus significantly affecting the debris removal efficiency of the raceway. This is another reason for the high mass losses of IS1/2, IS3/4 and BS. (5) Because of the narrow width of the pattern and less amount of wear debris needing to be transferred, the effect of the inside pits on the radial movement of wear debris is quite small. As a result, compared with the smooth group, the wear resistance of IS1/4 is significantly improved and its friction-reducing performance is also improved, due to the collection and storage capacity of pits. On the contrary, the outside pits of OS1/4 can suddenly and strongly interrupt the radial movement of wear debris. As a result, its nylon film left becomes thicker or even stacked locally (see Figure 5a) and its friction-reducing effect even worsens slightly for the high COF between nylon and steel. However, due to the protection of nylon film, its anti-wear performance is greatly improved instead. (6) The real tribological properties of pit textured cylindrical roller thrust bearings (both partially and entirely) with self-lubricating nylon cages under dry condition cannot be predicted at all and mainly depend on the combination of these factors: the area ratio of textured raceway, dimensions of pits, surface contact stresses, “edge crushing” phenomenon, loads (i.e., axial force, rotating speed), nylon film, shape of cage pockets and so on [33].

5. Conclusions

Through the comprehensive analysis of the obtained experimental and characterization data, the following conclusions could be drawn:

- (1) Nylon cages can ensure the continuous operation (≥ 5 h) of cylindrical roller thrust bearings under an axial load of 2600 N and a low rotating speed of 250 RPM, without any lubricant. The influence of outside-distributed groups (OS1/4, OS1/2 and OS3/4) on the friction and wear properties of bearings with self-lubricating nylon cages is significant under dry condition and that of inside-distributed groups is relatively small.
- (2) The friction-reducing effect and wear resistance of the full textured group (FP) is not the best, but it can still provide an acceptably comprehensive performance; compared with the smooth group, its average COF decreases by 19.37% and its wear loss decreases by 28.05%.
- (3) For those local-distributed patterns, IS1/4, OS1/2 and OS3/4 can provide positive wear resistance and friction-reducing performance. BS can provide well friction-reducing performance similar to that of FP, but its anti-wear behavior is quite poor. The result of OS1/4 is the opposite of BS. In this work, OS3/4 can provide the best comprehensive friction-reducing and anti-wear properties. Compared with the data of the smooth reference, its average COF and wear loss can be reduced by 37.68% and 38.85%, respectively.

Author Contributions: Conceptualization, R.L.; methodology, R.L.; software, Y.C.; validation, Y.C. and C.Z.; formal analysis, M.W.; investigation, C.Z.; resources, Z.J.; data curation, M.W.; writing—original draft preparation, Y.C.; writing—review and editing, R.L.; visualization, Y.C.; supervision, Z.J.; project administration, Z.J.; funding acquisition, R.L. All authors have read and agreed to the published version of the manuscript.

Funding: This research was funded by the Scientific Research Fund of Liaoning Provincial Education Department (No. LJKMZ20220800), the Natural Science Foundation of Liaoning province (No. 2019-MS-258), the National Natural Science Foundation of China Young Scientist Fund (No. 51901141).

Data Availability Statement: The data presented in this study are available on request from the corresponding author.

Acknowledgments: We would like to express our gratitude to Xuanying Du for providing language support in this paper.

Conflicts of Interest: The authors declare that there are no conflict of interest regarding the publication of this paper.

References

1. Bonse, J.; Kirner, S.V.; Griepentrog, M.; Spaltmann, D.; Krüger, J. Femtosecond Laser Texturing of Surfaces for Tribological Applications. *Materials* **2018**, *11*, 801. [[CrossRef](#)] [[PubMed](#)]
2. Zhao, C.; Long, R.S.; Zhang, Y.M.; Wang, Y.B.; Wang, Y.Y. Influence of characteristic parameters on the tribological properties of vein-bionic textured cylindrical roller thrust bearings. *Tribol. Int.* **2022**, *175*, 107861. [[CrossRef](#)]
3. Boidi, G.; Tertuliano, I.S.; Profito, F.J.; De Rossi, W.; Machado, I.F. Effect of laser surface texturing on friction behaviour in elastohydrodynamically lubricated point contacts under different sliding-rolling conditions. *Tribol. Int.* **2020**, *149*, 105613. [[CrossRef](#)]
4. Grützmacher, P.G.L.; Rosenkranz, A.L.; Szurdak, A.L.; Grüber, M.L.; Gachot, C.L.; Hirt, G.L.; Mücklich, F. Multi-scale surface patterning—an approach to control friction and lubricant migration in lubricated systems. *Ind. Lubr. Tribol.* **2019**, *71*, 1007–1016. [[CrossRef](#)]
5. Gropper, D.; Wang, L.; Harvey, T.J. Hydrodynamic lubrication of textured surfaces: A review of modeling techniques and key findings. *Tribol. Int.* **2016**, *94*, 509–529. [[CrossRef](#)]
6. Gachot, C.; Rosenkranz, A.; Hsu, S.M.; Costa, H.L. A critical assessment of surface texturing for friction and wear improvement. *Wear* **2017**, *372–373*, 21–41. [[CrossRef](#)]
7. Marian, M.; Grützmacher, P.; Rosenkranz, A.; Tremmel, S.; Mücklich, F.; Wartzack, S. Designing surface textures for EHL point-contacts-Transient 3D simulations, meta-modeling and experimental validation. *Tribol. Int.* **2019**, *137*, 152–163. [[CrossRef](#)]
8. Morales-Espeje, G.E.; Gabelli, A. Rolling bearing performance rating parameters: Review and engineering assessment. *Proc. Inst. Mech. Eng. Part J. Eng. Tribol.* **2020**, *234*, 3064–3077.
9. König, F.; Rosenkranz, A.; Grützmacher, P.G.; Mücklich, F.; Jacobs, G. Effect of single- and multi-scale surface patterns on the frictional performance of journal bearings—A numerical study. *Tribol. Int.* **2020**, *143*, 106041. [[CrossRef](#)]
10. Rosenkranz, A.; Grützmacher, P.G.; Gachot, C.; Costa, H.L. Surface Texturing in Machine Elements-A Critical Discussion for Rolling and Sliding Contacts. *Adv. Eng. Mater.* **2019**, *21*, 1900194. [[CrossRef](#)]
11. Rosenkranz, A.; Grützmacher, P.G.; Murzyn, K.; Mathieu, C.; Mücklich, F. Multi-scale surface patterning to tune friction under mixed lubricated conditions. *Appl. Nanosci.* **2021**, *11*, 751–762. [[CrossRef](#)]
12. Rosenkranz, A.; Costa, H.L.; Baykara, M.Z.; Martini, A. Synergetic effects of surface texturing and solid lubricants to tailor friction and wear—A review. *Tribol. Int.* **2021**, *155*, 106792. [[CrossRef](#)]
13. Kovalchenko, A.; Ajayi, O.; Erdemir, A.; Fenske, G.; Etsion, I. The effect of laser surface texturing on transitions in lubrication regimes during unidirectional sliding contact. *Tribol. Int.* **2005**, *38*, 219–225. [[CrossRef](#)]
14. Etsion, I.; Sher, E. Improving fuel efficiency with laser surface textured piston rings. *Tribol. Int.* **2009**, *42*, 542–547. [[CrossRef](#)]
15. Etsion, I. Surface texturing for in-cylinder friction reduction. *Tribol. Dyn. Engine Powertrain* **2010**, 458–470e.
16. Tala-Ighil, N.; Maspeyrot, P.; Fillon, M.; Bounif, A. Effects of surface texture on journal-bearing characteristics under steady-state operating conditions. *Proc. Inst. Mech. Eng. Part J. Eng. Tribol.* **2007**, *221*, 623–633. [[CrossRef](#)]
17. Rodrigues, G.W.; Bittencourt, M.L. Surface virtual texturing of the journal bearings of a three-cylinder ethanol engine. *Ind. Lubr. Tribol.* **2020**, *72*, 1059–1073. [[CrossRef](#)]
18. Wu, Z.P.; Nguyen, V.; Le, V.; Le, X.; Bui, V. Design and optimization of textures on the surface of crankpin bearing to improve lubrication efficiency and friction power loss of engine. *Proc. Inst. Mech. Eng. Part J. Eng. Tribol.* **2021**, *235*, 1139–1149. [[CrossRef](#)]
19. Jin, J.; Chen, X.C.; Fu, Y.Y.; Chang, Y.H. Optimal design of the slip-texture on a journal-bearing surface. *Ind. Lubr. Tribol.* **2021**, *73*, 230–237. [[CrossRef](#)]
20. Sharma, S.; Sharma, A.; Jamwal, G.; Awasthi, R.K. The effect of v-shape protruded and dimple textured on the load-carrying capacity and coefficient of friction of hydrodynamic journal bearing: A comparative numerical study. *Proc. Inst. Mech. Eng. Part J. Eng. Tribol.* **2021**, *235*, 997–1011. [[CrossRef](#)]
21. Morris, N.; Leighton, M.; De la Cruz, M.; Rahmani, R.; Rahnejat, H.; Howell-Smith, S. Combined numerical and experimental investigation of the micro-hydrodynamics of chevron-based textured patterns influencing conjunctive friction of sliding contacts. *Proc. Inst. Mech. Eng. Part J. Eng. Tribol.* **2015**, *229*, 316–335. [[CrossRef](#)]
22. Rahmani, R.; Rahnejat, H. Enhanced performance of optimised partially textured load bearing surfaces. *Tribol. Int.* **2018**, *117*, 272–282. [[CrossRef](#)]
23. Vlădescu, S.C.; Fowell, M.; Mattsson, L.; Reddyhoff, T. The effects of laser surface texture applied to internal combustion engine journal bearing shells—An experimental study. *Tribol. Int.* **2019**, *134*, 317–327. [[CrossRef](#)]
24. Rosenkranz, A.; Stratmann, A.; Gachot, C.; Burghardt, G.; Jacobs, G.; Mücklich, F. Improved Wear Behavior of Cylindrical Roller Thrust Bearings by Three-Beam Laser Interference. *Adv. Eng. Mater.* **2016**, *18*, 854–862. [[CrossRef](#)]

25. Long, R.S.; Zhao, C.; Jin, Z.H.; Zhang, Y.M.; Pan, Z.; Sun, S.N.; Gao, W.H. Tribological Behavior of Dents textured Rolling element Bearings under Starved Lubrication. *Ind. Lubr. Tribol.* **2021**, *73*, 971–979. [[CrossRef](#)]
26. Long, R.S.; Shang, Q.Y.; Jin, Z.H.; Zhang, Y.M.; Ju, Z.C.; Li, M.H. Tribological behavior of laser textured rolling element bearings under starved lubrication. *Ind. Lubr. Tribol.* **2022**, *74*, 453–462. [[CrossRef](#)]
27. Long, R.S.; Pan, Z.; Jin, Z.H.; Zhang, Y.M.; Sun, S.N.; Wang, Y.Y.; Wang, Y.B.; Li, M.H. Tribological behavior of grooves textured thrust cylindrical roller bearings under dry wear. *Adv. Mech. Eng.* **2021**, *13*, 16878140211067284. [[CrossRef](#)]
28. Long, R.S.; Zhao, C.; Zhang, Y.M.; Wang, Y.B.; Wang, Y.Y. Effect of vein-bionic surface textures on the tribological behavior of cylindrical roller thrust bearing under starved lubrication. *Sci. Rep.* **2021**, *11*, 21238. [[CrossRef](#)]
29. Wang, Y.Y.; Zhang, Y.M.; Long, R.S. Influence of Pits on the Tribological Properties and Friction-Induced Vibration Noise of Textured Tapered Roller Bearings. *Tribol. Trans.* **2022**, 1–11. [[CrossRef](#)]
30. Vidyasagar, K.E.C.; Pandey, R.K.; Kalyanasundaram, D. An exploration of frictional and vibrational behaviors of textured deep groove ball bearing in the vicinity of requisite minimum load. *Friction* **2021**, *9*, 1749–1765. [[CrossRef](#)]
31. Grützmacher, P.G.; Suarez, S.; Tolosa, A.; Gachot, C.; Song, G.C.; Wang, B.; Presser, V.; Mücklich, F.; Anasori, B.; Rosenkranz, A. Superior Wear-Resistance of Ti3C2Tx Multilayer Coatings. *ACS Nano* **2021**, *15*, 8216–8224. [[CrossRef](#)] [[PubMed](#)]
32. Marian, M.; Feile, K.; Rothhammer, B.; Bartz, M.; Wartzack, S.; Seynstahl, A.; Tremmel, S.; Krauß, S.; Merle, B.; Böhm, T.; et al. Ti3C2Tx solid lubricant coatings in rolling bearings with remarkable performance beyond state-of-the-art materials. *Appl. Mater. Today* **2021**, *25*, 101202. [[CrossRef](#)]
33. Gao, S.; Han, Q.K.; Zhou, N.N.; Zhang, F.B.; Yang, Z.H.; Chatterton, S.; Pennacchi, P. Dynamic and wear characteristics of self-lubricating bearing cage: Effects of cage pocket shape. *Nonlinear Dynam.* **2022**, *110*, 177–200. [[CrossRef](#)]
34. Grützmacher, P.G.; Rosenkranz, A.; Rammacher, S.; Gachot, C.; Frank, M. The influence of centrifugal forces on friction and wear in rotational sliding. *Tribol. Int.* **2017**, *116*, 256–263. [[CrossRef](#)]

Disclaimer/Publisher's Note: The statements, opinions and data contained in all publications are solely those of the individual author(s) and contributor(s) and not of MDPI and/or the editor(s). MDPI and/or the editor(s) disclaim responsibility for any injury to people or property resulting from any ideas, methods, instructions or products referred to in the content.